UNCLASSIFIED

AD NUMBER ADB332554 LIMITATION CHANGES TO: Approved for public release; distribution is unlimited. FROM: Distribution authorized to DoD only; Administrative/Operational Use; JAN 1944. Other requests shall be referred to Office of Scientific Research and Development, Washington, DC, 2031. Pre-dates formal DoD distribution statements. Treat as DoD only. **AUTHORITY** OTS index dtd Jun 1947

UNGLASSIFIED

Tolch Thomas

NATIONAL DEFENSE RESEARCH COMMITTEE

ARMOR AND ORDNANCE REPORT NO. A-244 (CSRD NO. 3207)

DIVISION 2

PRELIMINARY EXPERIMENTS ON THE PROPAGATION
OF PLASTIC DEFORMATION

A Revision of NDRC Report A-33 (CSRD No. 380)

by

Pol E. Duwez

20071002057

UNGLASSIFIED

Best Available Copy

Сору No. 50

7-9586 c

DECHNICAL INFORMATION BRANDED RESEARCH CENTER ABERDEEN PROVING GROUND



NATIONAL DEFENSE RESEARCH COMMITTEE ARMOR AND ORDNANCE REPORT NO. A-244 (OSRD NO. 3207) DIVISION 2

PRELIMINARY EXPERIMENTS ON THE PROPAGATION OF PLASTIC DEFORMATION

A Revision of NDRC Report A-33 (OSRD No. 300)

by

Pol E. Duwez

Approved on January 18, 1944 for submission to the Division Chief

Approved on February 2, 1944 for submission to the Committee New P. White

Merit P. White, Secretary Division 2

Bunham Kelly

Burnham Kelly
Special Assistant to the Chief

oural Defense and Offense

D-0586 P1 nobu

Preface

The work described in this report is pertinent to the projects designated by the Navy Department Liaison Officer as NO-11 and NS-109 and to Division 2 project P2-303.

This work was carried out and reported by the California Institute of Technology under Contract OEMsr-348.

The author wishes to acknowledge the suggestions of C. Zener and J. H. Hollomon who pointed out in NDRC Memorandum A-37M (OSRD No. 659) that in von Kármán's theory of the propagation of plastic deformation the stress that appeared in the equations was in reality the apparent, or engineering, stress and not the true stress as had been assumed. They showed that with this change the experimental results herein reported were in agreement with the theory. Appropriate changes have accordingly been made in this revision of NDRC Report A-33 (OSRD No. 380).

Initial distribution of copies of this report

Nos. 1 to 25, inclusive, to the Office of the Secretary of the Committee for distribution in the usual manner;

No. 26 to R. C. Tolman, Vice Chairman, NDRC;

No. 27 to R. Adams, Member, NDRC;

No. 28 to F. B. Jewett, Member, NDRC;

No. 29 to J. E. Burchard, Chief, Division 2;

No. 30 to W. Bleakney, Deputy Chief, Division 2;

No. 31 to W. F. Davidson, Office of the Chairman, NDRC;

No. 32 to R. A. Beth, Member, Division 2;

No. 33 to H. L. Bowman, Member, Division 2;

No. 34 to C. W. Curtis, Member, Division 2;

No. 35 to C. W. Lampson, Member, Division 2;

No. 36 to W. E. Lawson, Member, Division 2;

No. 37 to F. Seitz, Jr., Member, Division 2;

No. 38 to A. H. Taub, Member, Division 2;

No. 39 to E. B. Wilson, Jr., Member, Division 2;

Nos. 40 and 41 to R. J. Slutz, Technical Aide, Division 2;

No. 42 to Army Air Forces (Brig. Gen. B. W. Chidlaw);

Nos. 43 and 44 to Corps of Engineers (Maj. W. J. New);

No. 45 to Ordnance Department (Col. S. B. Ritchie);

No. 46 to M. P. White Technical Aide Division 2;

Nos. 47 and 48 to Watertown Arsenal (Col. H. H. Zornig, C. Zener);

No. 49 to Frankford Arsenal (Lt. Col. C. H. Greenall);

Nos. 50 and 51 to Aberdeen Proving Ground (R. H. Kent, O. Veblen);

No. 52 to Watervliet Arsenal (Col. S. L. Conner);

Nos. 53 and 54 to Bureau of Ordnance (Comdr. T. J. Flynn, A. Wertheimer);

No. 55 to Commanding Officer, U.S. Naval Proving Ground;

No. 56 to David Taylor Model Basin (Capt. W. P. Roop);

Nos. 57 and 58 to Bureau of Ships (Lt. Comdr. R. W. Goranson, E. Rassman);

No. 59 to Bureau of Yards and Docks (War Plans Division);

No. 60 to U.S. Naval Research Laboratory (R. Gunn);

No. 61 to Rear Adm. R. S. Holmes, California Institute of Technology;

No. 62 to N. M. Newmark, Consultant, Division 2;

No. 63 to Th. von Karmán, Consultant, Division 2;

No. 64 to A. Nadai, Consultant, Division 2;

No. 65 to P. W. Bridgman, Consultant, Division 2;

No. 66 to L. H. Adams, Chief, Davision 1;

No. 67 to E. L. Rose, Member, Davision 1;

No. 68 to D. S. Clark, California Institute of Technology;

No. 69 to P. E. Duwez, California Institute of Technology;

The NDRC technical reports section for armor and ordnance edited this report and prepared it for duplication.

CONTENTS

		Page
Abstract		. 1
Section		
1.	Experimental setup	2
2.	Static stress-strain curve for the specimen used	3
3.	Measurements of the distribution of the strain along the specimen	4
4.	Results of the high-velocity impact tests	9
5.	Conclusions	19
	List of Figures	
Figure		Page
1.	Experimental device used to stop the impact after a given deformation of the specimen is reached	5
2:	Static apparent stress-strain curve for copper wire 0.071 in. in diameter	6
3,4.	Strain versus velocity of propagation as calculated from the static stress-strain curve	7
5.	Variation of the strain with the impact velocity	8
6.	Distribution of the elongation along the specimen	11
7.	Linear portions of the curves of Fig. 6	12,
8.	Distribution of the strain along the specimen	12
9.	Distribution of the elongation along the specimen	14
10,11.	Distribution of the strain along the specimen	15
12.	Plastic waves computed from theory and measured experimentally	16
13.	Same curve as Fig. 3 with experimental results added.	16

PRELIMINARY EXPERIMENTS ON THE PROPAGATION OF PLASTIC DEFORMATION

Abstract

In a recent report, von Kármán develops a theory of the propagation of plastic deformation in solids that may open the way to a systematic interpretation of a great many impact and penetration problems in which plastic deformations of beams, plates and armor are involved. The present report describes experiments that have been made with the object of testing the assumptions of the theory and that provide data on (i) the existence of a plastic wave front of a given amplitude. (ii) the relation between the velocity of impact and the amplitude of the plastic wave front, and (iii) the shape of the plastic wave and the velocity of propagation of the plastic front. The experiments show that the theory is able to describe, along general lines, the process of the propagation of deformation in solids. In particular, the theoretically predicted relation between the velocity of impact and the resulting maximum plastic deformation checks quite well with the experiments. The actual shape of the plastic wave is found to be at some variance with the theoretically obtained curves and, hence, needs further explanation.

The object of the experiments described in this report is to check the formulas established in von Kármán's theory of the propagation of plastic deformation in solids. The verification deals chiefly with the following three points.

- (i) The existence of a plastic wave front of a given amplitude.
- (ii) The relation between the amplitude ε_1 of the plastic wave front and the velocity of impact v_1 , namely,

$$v_1 = \int_0^{\varepsilon_1} \sqrt{(d\sigma/d\varepsilon)/\rho} \ d\varepsilon, \qquad (1)$$

^{1/} Th. von Kármán, On the propagation of plastic deformation in solids, NDRC Report A-29 (OSRD No. 365), Jan. 1942.

^{2/} This is Eq. (11), ref. 1.

where $\underline{\sigma}$ is the apparent or engineering stress, $\underline{\varepsilon}$ is the strain and $\underline{\varepsilon}$ is the mass density of the solid material.

(iii) The distribution of the plastic strain \underline{s} between the plastic and the elastic front as given by the formula

$$d\sigma/d\varepsilon = \rho x^2/t^2, \qquad (2)$$

where $ds/d\epsilon$ is the modulus of deformation, \underline{x} is the distance from the end of the wire to the point under consideration, and \underline{t} is the time.

1. Experimental setup

The testing machine employed in this investigation was available in the Impact Testing Laboratory at the California Institute of Technology under the direction of D. S. Clark. In this machine, the impact is produced by a hammer that falls between two vertical rails and that is accelerated by prestretched rubber bands. The maximum velocity attainable is approximately 200 ft/sec. The velocity is measured by a suitable electric device.

The specimen used was an annealed copper wire about 100 in. long and 0.071 in. in diameter. On every specimen equidistant marks were made with 1-in. spacing. After the test, the plastic strain was determined by measuring the displacement of each mark. In order to observe the propagation of the plastic wave while it travels up the wire, a series of experiments was made, all with the same velocity but with the impact stopped after different time intervals which varied from 0.4 to 4 millisec.

^{3/} Eq. (9), ref. 1.

To control the duration of impact, the following device was employed. The bottom end of the wire is attached to a rigid piece A (Fig. 1). At B is a vertical rod that rests on the bottom frame of the machine. The upper end of this rod fits loosely into the tubular part of A. When the hammer H hits the piece A, the specimen elongates until A reaches the rod B. The piece A contains a circular notch N, and the rim of A breaks off at this notch after A has traveled the distance D and comes to rest on the rod B. The purpose of this arrangement is to allow the hammer to continue to move downward and also to dissipate some of its remaining kinetic energy. However, no kinetic energy is transferred to the specimen after A reaches B. The time of impact is therefore the distance D divided by the velocity of the hammer during the process of elongation.

2. Static stress-strain curve for the specimen used

The static stress-strain curve for the copper used in the impact tests is shown in Fig. 2. The specimen employed in the static test was a 20-in. length of the wire used for the impact experiments. The stress plotted in Fig. 2 is the apparent stress, which is the load divided by the initial cross-sectional area.

From the afore-mentioned static stress-strain curve the value of $d\sigma/d\epsilon$ was calculated as a function of ϵ and then a curve was plotted showing the quantity

as a function of $\underline{\varepsilon}$. This quantity, according to the theory, gives the velocity of propagation \underline{c} , corresponding to each strain $\underline{\varepsilon}$. In Fig. 3

the value of <u>c</u> derived from the static stress-strain curve is plotted as a function of the strain <u>E</u>. Figure 4 represents the continuation of the curve of Fig. 3 up to the velocity of the elastic front. From these curves the value of the quantity

$$\mathbf{v_1} = \int_0^{\varepsilon_1} \mathrm{cd}\varepsilon \tag{3}$$

can be calculated for each value of \mathcal{E}_1 , where \mathbf{v}_1 is the velocity of impact corresponding to a plastic front of amplitude \mathcal{E}_1 . The curve \mathbf{v}_1 versus \mathcal{E}_1 is shown in Fig. 5. This curve reaches an end at the point \mathcal{E}_1 = 16 percent, \mathbf{v}_1 = 150 ft/sec. The impact velocity of 150 ft/sec is therefore the "critical velocity" for this material. An impact with a higher velocity must produce an instantaneous breakdown of the specimen.

3. Measurements of the distribution of the strain along the specimen

As mentioned in Sec. 1, marks were made on the specimen at intervals of 1 in. The distance between the origin and each mark is denoted by $x_1, x_2, \ldots x_n$, respectively. After the test the new distances between the origin and the marks were measured; these distances are denoted by $x_1', x_2', \ldots x_n'$. When the differences $x_n' - x_n$ are plotted as a function of \underline{x} , curves such as those shown in Fig. 6 are obtained. The sequence of curves corresponds to increasing durations of impact. The slope of the curves at any point gives the value of the permanent strain at that point. This way of measuring the strain has been found to be the most practical one. It was not found necessary to make the distinction between permanent strain and actual strain, because the elastic recovery was relatively too small to be taken into consideration.

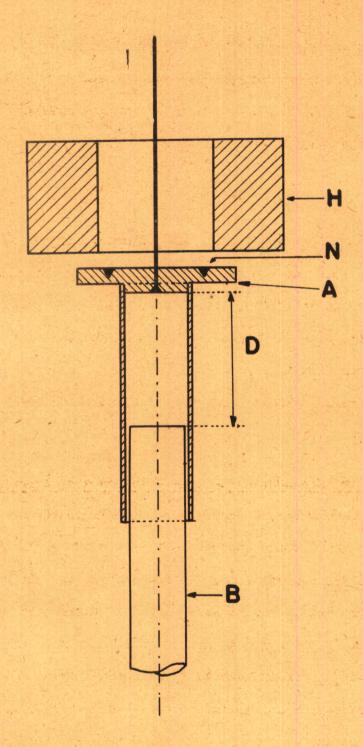


Fig. 1. Experimental device used to stop the impact after a given deformation of the specimen is reached.

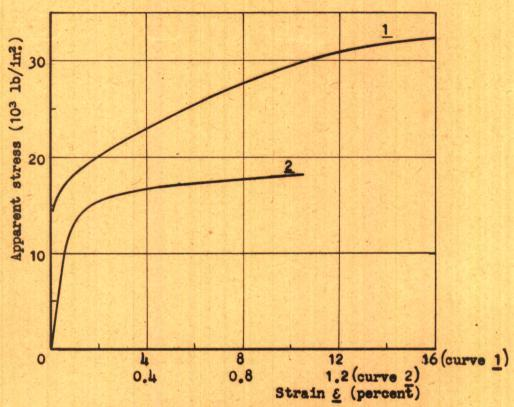


Fig. 2. Static apparent stress-strain curve for copper wire 0.071 in. in diameter. Curve 2 is the portion of the same stress-strain curve with an enlarged scale for the strain.

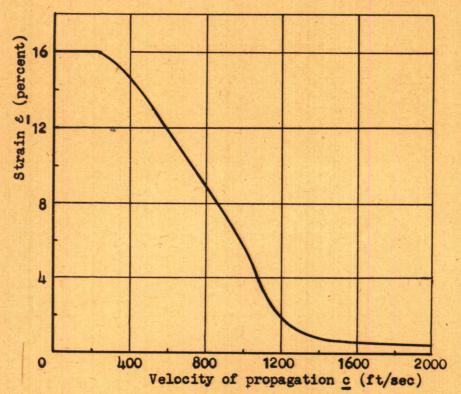


Fig. 3. Strain $\underline{\varepsilon}$ versus velocity of propagation \underline{c} , as calculated from the static stress-strain curve.

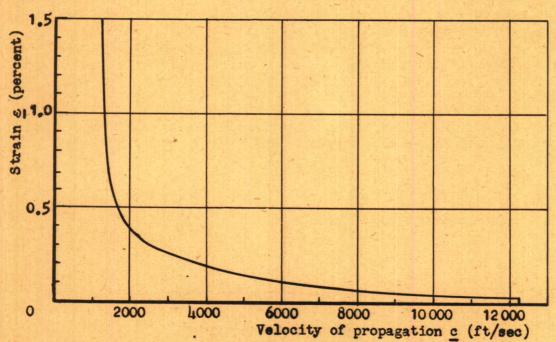
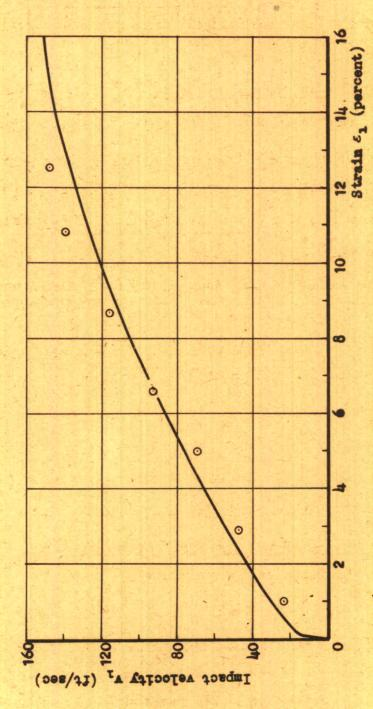


Fig. 4. Continuation of the curve of Fig. 3 up to the elastic point.



solid line Fig. 5. Variation of the strain & with the impact velocity vi: computed theoretically; circles measured experimentally.

4. Results of the high-velocity impact tests

The results are given in three separate subsections -- (i), (ir) and (iii) -- in order to show to what extent they agree with the three principal theoretical results which were expressed at the beginning of this report.

(i) Existence of a plastic wave front. -- The first series of tests was made in order to show that the amplitude of the plastic front is a function of the velocity of impact alone. This amplitude remains constant while the elastic front and the plastic front travel along the specimen. In these particular experiments, the velocity of impact was always 92.50 ft/sec, but the durations of the impact were varied. To control the duration of impact, the two pieces A and B shown in Fig. 1 must be placed at a proper distance apart. It is rather difficult to measure this distance accurately. For that reason the approximate duration of impact t was calculated from the total elongation D, measured on the specimen after the test, and the velocity v1 of the hammer after impact; the formula used is $t = D/v_1$. The velocity v_1 of the hammer after impact was determined from the measured value of the velocity of the hammer immediately before the impact which is multiplied by the ratio $m_{H}/(m_{H}+m_{A})$, where m_{H} and m_{A} denote the masses of the hammer and the piece A, respectively.

Figure 6 shows the distribution of the elongation $x_n' - x_n$ along the wire; the approximate duration of impact is indicated on each curve and is also given in Table I. The determination of the duration of impact and the computation of the velocity of propagation \underline{c} is discussed in Sec. 4(iii). The slopes of the straight portions of all the

curves shown in Fig. 6 are the same. Figure 7 shows the actual readings and their deviations from a straight line for each test. The curves in Fig. 8 — obtained by computing the derivatives of the functions shown in Fig. 6 — give the distribution of the strain along the specimen. We may therefore conclude that a plastic front of a given amplitude \mathcal{E}_1 is revealed by the experiments as predicted from the theory.

Table I. Tests in which the velocity of impact v₁ was always 92.50 ft/sec but the durations of impact t were different.

D, total elongation of the specimen;
d, distance traveled by the front of the plastic wave and measured on the curves of rig. o;

t[= D/v], approximate duration of impact (millisec);
c[= d/t], approximate velocity of propagation of the plastic wave.

$(\underline{\underline{n}}_{\cdot})$	(in.)	(10 ^{-3 t} sec)	c (ft/sec)
0.46 0.925 1.14 1.81 2.50 4.17	4.4 9.45 12.4 17.8 26.4 41.5	0.415 0.834 1.03 1.63 2.255 3.76	890 945 1000 910 975 920
		Mean Value	940

(ii) Relation between the velocity of impact and the amplitude of the plastic wave front. — In this series of tests, the velocity of impact was varied from one test to the other. The total elongation was not necessarily the same for all the tests. The stopping device was adjusted in such a manner that during the impact the plastic front traveled a distance of between 20 and 40 in. Figure 9 again shows the

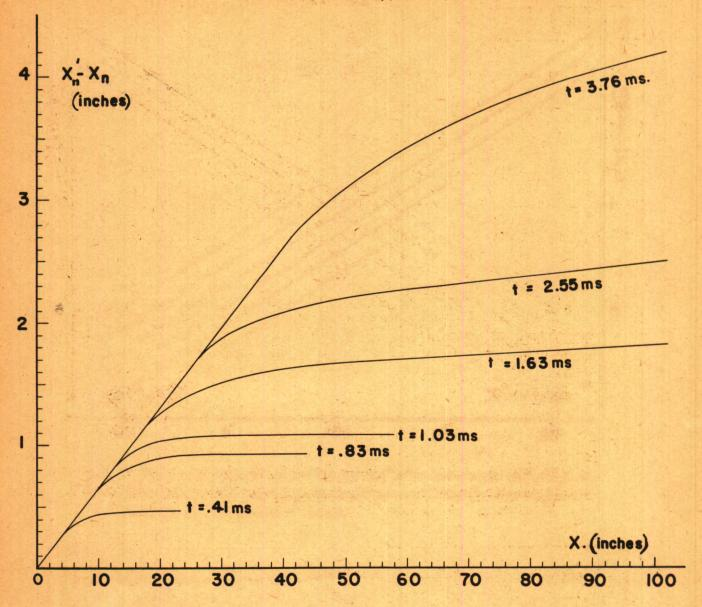


Fig. 6. Distribution of the elongation $X'_n - X_n$ along the specimen. Speed of impact, 92.5 ft/sec. The duration of impact (millisec) is indicated on each curve.

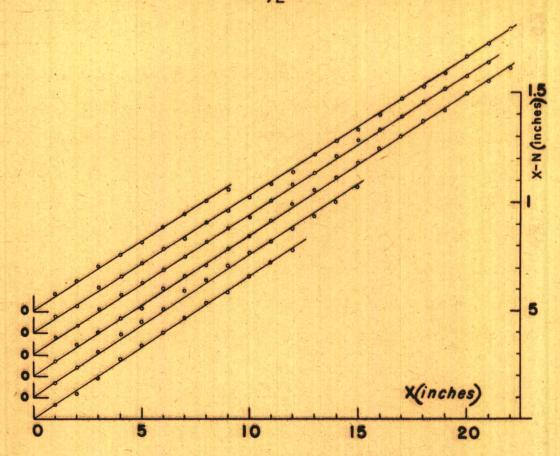


Fig. 7. Linear portions of the curves of Fig. 6, showing the actual readings and their deviations from a straight line.

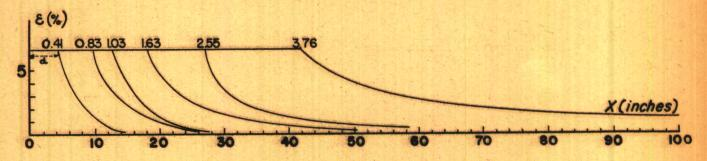


Fig. 8. Distribution of the strain & along the specimen. Speed of impact, 92.5 ft/sec. The duration of impact (millisec) is indicated on each curve.

elongations x,' - x, at points on the specimen corresponding to the distances x from the origin. The slope of the straight-line portion of each curve gives the amplitude of the plastic front for each velocity of impact. Figure 10 gives the distribution of the strain along the specimen in each case. The experimental values of E, corresponding to each velocity tested are listed in Table II. For comparison with the theory, the experimental values are plotted as points in Fig. 5, whereas the solid curve represents the result of the theoretical computation. The agreement between the experimental results and

Table II. Tests in which the velocities of impact v, were varied.

V1, velocity of impact;

E, amplitude of the plastic wave (percent);

D, total elongation of the specimen; distance traveled by the front of the plastic wave and

measured on the curves of Fig. 10; $t[=D/v_1]$, approximate duration of impact (millisec);

c[= d/t], approximate velocity of propagation of the plastic wave.

v ₁ (ft/sec)	$oldsymbol{arepsilon}_{ ext{i}}$ (percent)	<u>D</u> (in.)	<u>d</u> (in.)	(10 ^{-3^t} sec)	c (ft/sec)
23.1 46.2 69.4 92.5 115.0 139.0 148.0 171.0	1.0 2.9 5.0 6.6 8.7 10.8 12.5	0.47 0.82 2.81 1.81 2.14 3.24 2.49 Rupt	25.0 20.0 40.5 17.8 16.0 17.0 10.5 ure	1.70 1.47 3.37 1.63 1.55 1.94 1.40	1230 1130 1000 910 860 73 6 630

the predetermined curve is fairly good. The highest velocity of impact used was 171 ft/sec. For that velocity, the specimen broke within the first inch, indicating that a velocity of 171 ft/sec is above the critical velocity, as predicted by the theory. The distribution of the

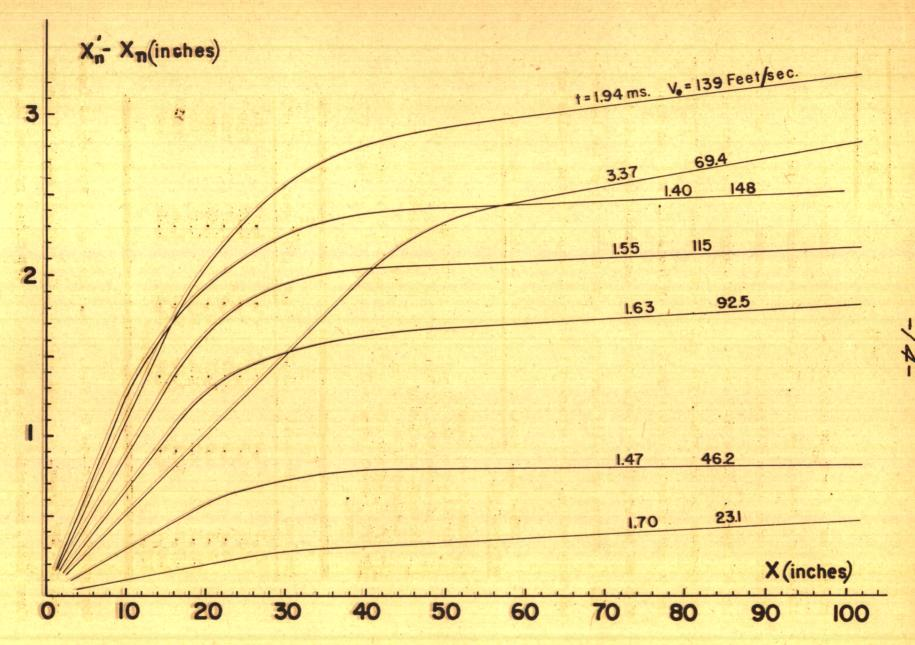


Fig. 9. Distribution of the elongation X'-Xn along the specimen. The velocity and duration of impact are indicated on each curve.



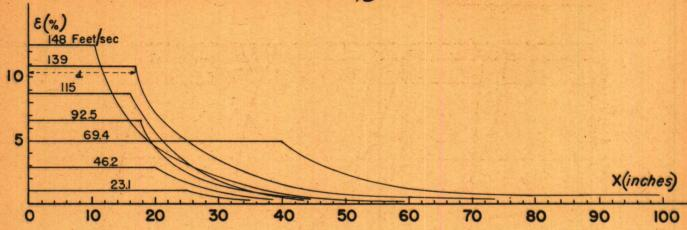


Fig. 10. Distribution of the strain & along the specimen. The speed of the impact (ft/sec) is indicated on each curve.

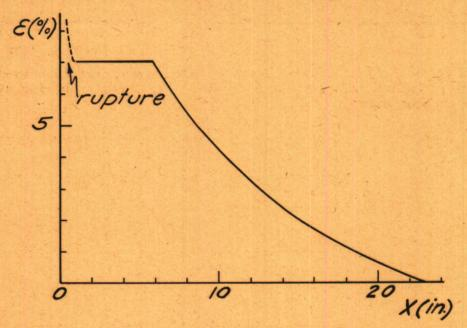


Fig. 11. Distribution of the strain along the specimen broken at a speed of impact of 171ft/sec. Rupture occured within lin from the end of the specimen, where the strain is about 50 percent.

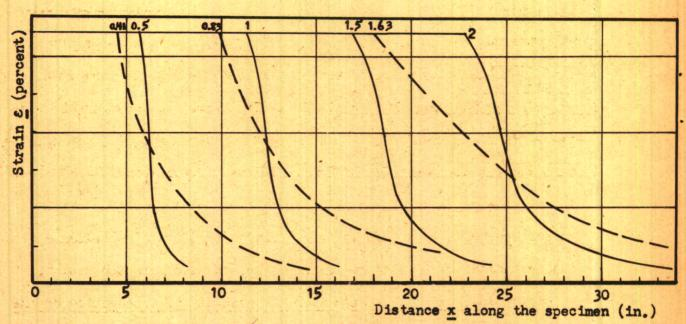


Fig. 12. Plastic waves computed from theory (solid curves) and measured (broken curves). Impact velocity, 92.5 ft/sec. The duration of impact (millisec) is indicated on each curve.

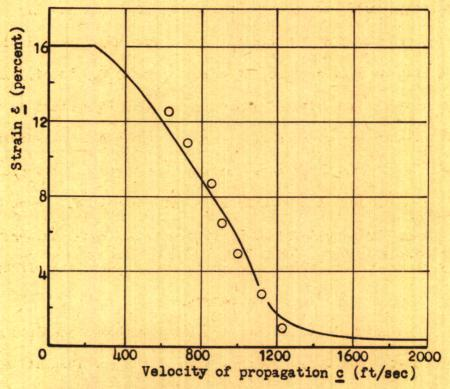


Fig. 13. Same curve as Fig. 3 with experimental results (dots) added.

strain along the specimen is shown in Fig. 11. It must be pointed out that, whereas the rupture occurs at the bottom end of the specimen, a plastic wave of relatively small intensity travels a considerable distance along the specimen, as shown by the curve in Fig. 11. It appears that the rupture required a relatively large time interval. The first inch of the specimen showed an elongation of about 50 percent; this corresponds to a time interval of 0.24 millisec. More experiments on the critical impact velocity are necessary to elucidate this point.

(iii) Shape of the plastic wave and velocity of propagation of the plastic front. — The distribution of the plastic strain ε along the wire between the plastic and elastic fronts may be calculated from Eq. (2), using the curves of Figs. 3 and 4. The solid curves in Fig. 12 represent theoretically computed amplitude distributions of a plastic wave after time intervals equal to 0.5, 1, 1.5 and 2 millisec; the assumed velocity of impact v_1 is 92.5 ft/sec and ε_1 is 6.6 percent. The dashed curves in Fig. 12 represent plots of the distribution of the strain for three tests made with a velocity of impact of 92.5 ft/sec. It is seen that the experimental and theoretical curves deviate considerably. This deviation is probably due to the inaccuracy in the value of the duration of impact, and to the perturbating effects wrought by the sudden stopping of the impact.

As pointed out in Sec. 4(i), the method of computing the duration of impact from the total extension of the specimen at the completion of the test is not quite correct. Additional theoretical work — done after these preliminary experiments were first published — has shown that after the hammer, which pulls the end of the wire with a constant

velocity, is stopped, the portion of the specimen that is in motion is not stopped instantaneously. During the deceleration period, the kinetic energy stored in the specimen is transformed into strain energy, and the total extension is larger than the distance D through which the hammer has been in contact with the specimen. No provision was made in the experimental setup to permit the end of the specimen to travel down after the hammer was stopped. The velocity of the end of the specimen, therefore, dropped suddenly from v, to 0 and this condition, as revealed by further theoretical considerations, leads to the initiation of a compressive wave in the specimen. It is very probable that such a compressive wave could not travel along a specimen of the type used for these experiments and evidence of localized buckling was found, chiefly in the tests made at high impact velocities. Accordingly, it is necessary to consider that all the velocities of propagation reported here which involve the measurement of the duration of impact are approximate.

The measured shapes of the plastic waves given in Fig. 12 are greatly influenced by the stopping effect and cannot logically be compared with the theoretical curves that represent the shape of the wave at a certain instant during impact. Further theoretical work has shown that the measured curves of strain distribution should be displaced to the right with respect to the computed curve, as shown in Fig. 12. The more complete theory also shows that the distance traveled by the maximum plastic strain \mathcal{E}_1 is slightly influenced by the stopping effect. This indicates that a rather good agreement should be observed between theoretical and experimental velocity of propagation of the strain \mathcal{E}_1 .

The values of these velocities have been plotted in Fig. 13, and the agreement is, as expected, fairly good.

In the original report (A-33), it was stated that the discrepancies between theory and experiments were probably due to the influence of the finite length of the specimen, the influence of the rate of strain on the stress-strain relation of the material (neglected in the theory) and the fact that the impact was not perfectly instantaneous. These three reasons were found later to be less influential than the stopping effect discussed in the present report.

5. Conclusions

It is seen that the theory is able to describe in general lines the process of the propagation of plastic deformation in solids. The theoretical relation established between the velocity of impact and the maximum plastic deformation produced by the same impact checks quite well with the experiments. The shape of the plastic wave is at some variance with the theoretically obtained curves. As shown by further theoretical and experimental research, these variances have been attributed primarily to the perturbation initiated after the impact has been stopped.